# Behaviour and critical failure modes of strip foundations on slopes under seismic and structural loading

Dhiraj Raj[1], Yogendra Singh[2] and Amir M. Kaynia[3]

[1]*Research Scholar, Department of Earthquake Engineering, Indian Institute Technology Roorkee, Roorkee 247-667, India, E-mail: dhirajraj.iitr@gmail.com*

[2]*Professor and Head, Department of Earthquake Engineering, Indian Institute Technology Roorkee, Roorkee 247-667, India (corresponding author), E-mail: yogendra.eq@gmail.com*

[3]*Technical Expert, Norwegian Geotechnical Institute, P.O. Box 3930 Ullevaal Stadion, 0806 Oslo, Norway, E-mail: amir.m.kaynia@ngi.no*

**Abstract:** This paper presents a numerical study on capacity envelopes of strip foundations placed on top and face of two typical soil slopes at different offset distances and subjected to earthquake effects considered using the pseudo-static method. The capacity is estimated using nonlinear 2D finite element limit analysis. Modified swipe and probe analyses are carried out to develop vertical force- moment (*V-M*) and vertical force- shear force (*V-H*) capacity envelopes. Characteristic features of these capacity envelopes, and critical failure modes of foundations on slopes are identified and compared with the foundations on flat ground. Relative influence of the soil and structure inertia on capacity envelope of foundation is also explored. It is found that the critical failure mode of a foundation on slope, subjected to gravity and seismic action depends on the effective column height of the structure. A comparison of the capacity envelopes of typical foundations with the corresponding reinforced concrete columns indicates that the foundation design methods of the current building codes cannot avoid premature failure of foundations on slopes, prior to columns.

**Keywords:** Capacity envelope; Slope-foundation interaction; Seismic Loading; Finite element limit analysis (FELA); Capacity design

## Introduction

In practice, foundations are often subjected to simultaneous vertical load ($V$), lateral shear ($H$) and bending moment ($M$) generated from the combined action of vertical (gravity) and lateral (wind or earthquake) loads. Most of the current standards and codes of practice (IS6403 1986; EN1997-1 2004; NCHRP 2010) use classical formulation for estimation of bearing capacity of shallow foundations (Terzaghi 1943) and recommend various correction factors to incorporate the effect of shear force and bending moment. The effect of shear force is taken into account with the help of load inclination factor, whereas the effect of bending moment is considered in terms of eccentricity of vertical load from the center of the foundation and through use of an effective width or area of the foundation. However, the capacity of foundations under general planar loading can be better dealt with using capacity envelope (or load interaction) method (Gourvenec and Randolph 2003; Gourvenec 2007a), which explicitly takes into account the interacting load components. This approach has also been incorporated by some of the advanced seismic design codes (EN1998-5 2004; NCHRP 2010; ASCE/SEI41-13 2014) by providing empirical capacity envelopes for some simple cases for foundations on flat ground.

A preliminary review of the behaviour of typical structures indicates that the moment acting on the foundation is actually related to the horizontal shear force and an effective height of the structure rather than the vertical load. Figure 1 illustrates the effective height of two typical structures. In case of a bridge pier, the effective height ($h$) is the vertical distance between the foundation and centre of mass of the bridge deck, as shown in Fig. 1(a). Whereas, for a moment resisting frame (MRF), the effective height depends on the deflected shape (double curvature under lateral load) of the column and can be considered as half of storey height, as shown in Fig. 1(b). The moment acting on the foundation can then be estimated as the product of shear force and effective height of the column/pier (i.e. $M = H \times h$).

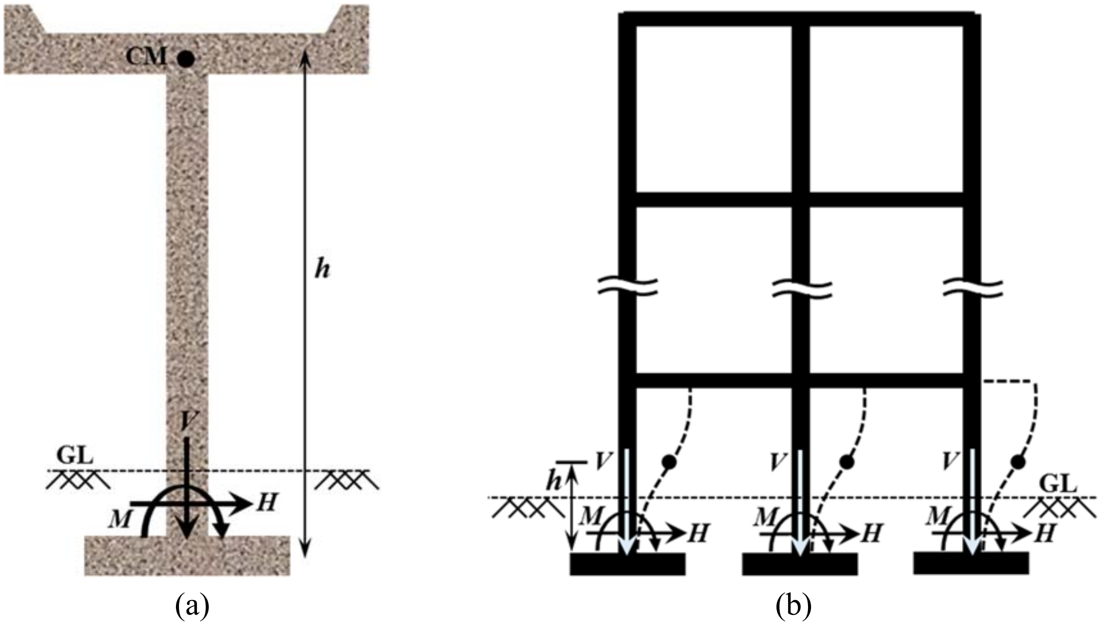


**Fig. 1.** Effective height of column/pier in typical structures: (a) A single pier bridge; (b) Moment resisting frame building

Analytical solutions as well as simple empirical equations are available for the calculation of the failure loads of shallow foundations placed on flat cohesive soil (Ukritchon et al. 1998; Taiebat and Carter 2000; Bransby 2001; Gourvenec and Randolph 2003; Yun and Bransby 2007; Gourvenec 2007a; Gourvenec 2008; Yilmaz and Bakir 2009; Taiebat and Carter 2010; Vulpe et al. 2014; Shen et al. 2016; Xiao et al. 2016), and on flat cohesionless soil (Nova and Montrasioa 1991; Gottardi and Butterfield 1993; Butterfield and Gottardi 1994; Gottardi and Butterfield 1995; Montrasioa and Nova 1997; Paolucci and Pecker 1997; Gottardi et al. 1999; Houlsby and Cassidy 2002; Loukidis et al. 2008; Krabbenhoft et al. 2012; Kim et al. 2014; Kim et al. 2014; Tang et al. 2014; Nguyen et al. 2015). Some experimental studies conducted on shallow foundations subjected to general planer loading have also been reported in the literature (Martin and Houlsby 2000; Govoni et al. 2010; Cocjin and Kusakabe 2013). However, most of the available studies deal with shallow foundations constructed on flat ground consisting of either purely cohesive, or purely cohesionless soils. A few studies are also available on evaluation of capacity envelope for shallow foundations placed on top of a slope. Georgiadis (2010) has performed a parametric study using finite element, upper bound plasticity, and stress field methods to examine the influence of a wide range of geometries (slope height, slope angle and normalized foundation distance) on the static capacity envelopes of foundations located on top of slopes. He considered undrained cohesive soil behavior and proposed an empirical equation for the capacity envelope. Baazouzi et al. (2016) conducted a study on vertical-horizontal load interaction diagram of shallow foundations placed on top of cohesionless slopes and found out that the shape of the interaction diagram depends on the slope angle and the distance of the foundation from the slope.

It has been found from the available literature that the capacity envelopes have not been studied for: (a) foundations located on face of slopes; (b) slopes consisting of $c$-$\phi$ soils; (c) foundations subjected to moment in combination with vertical load; and (d) slope-foundation systems subjected to seismic loading (considering the effect of soil mass inertia). Hence, in this article, an attempt is made to address all the above issues and understand the associated failure mechanisms. To this end, capacity envelopes are developed for strip foundations placed on top and face of the slopes consisting of homogenous $c$-$\phi$ soils, and located at different offset distances and subjected to seismic loads in addition to general planar loads. 2D nonlinear Finite Element (FE) models of slopes (of different geometry and soil properties) and foundations (of varying offset distance but fixed width) are developed using OptumG2 (2018) finite element limit analyses (FELA) software. The results thus obtained are presented in the form of normalized $V$-$M$ and $V$-$H$ interaction diagrams and are compared to identify the governing failure modes under different combinations of $V$, $H$, and $M$. The influence of effective structural height, offset distance and seismic loading on capacity envelopes and the resulting failure mode are explored in detail. Capacity design is a crucial step in the modern earthquake resistant design practice, which consists of proportioning of different components of structure with a pre-decided hierarchy of strength to achieve a desired yield pattern. In the later part of the present study, capacity envelopes of typical foundations on slopes designed according to selected standards and literature are compared with capacity curves of the corresponding reinforced concrete (RC) columns supported on these foundations with the objective of examining the relative hierarchy of strength between typical columns and foundations.

## Problem Statement

In the present study, two homogeneous slopes having same height (40 m from the slope toe) and inclined at angles, $\beta = 20°$ and $30°$ from horizontal, have been considered consisting of dry 'stiff clay' and 'dense sand' soil, respectively, following Fotopoulou and Pitilakis (2013) (see Table 1). The static factor of safety of the 20° and 30° slopes was found to be 2.3 and 2.0, respectively, using finite element limit analyses (FELA) based on strength reduction technique. Both slopes were found to become unstable at a horizontal seismic coefficient, $\alpha_h \approx 0.36g$ (where, $g$ is acceleration due to gravity) using the pseudo-static approach. A rigid rough strip foundation having width, $B = 2$ m has been considered on the slopes at two different locations: on top of the slope and at mid-face of the slope as shown in Fig. 2. For the purpose of comparisons, the foundation is also considered to be located on the surface of flat ground with the same soil properties. The figure also shows the strip foundation under the action of combined planar ($V$, $H$ and $M$) and seismic loading ($\alpha_h$). The sign convention for applied loads and moment follows inside right hand thumb rule (Butterfield et al. (1997). The foundation has also been considered at three different offsets distances, $b/B = 0$, 1 and 2, where $b$ is the distance of the foundation edge from the slope face. The strip foundation located at 'Top' is placed at the surface of the ground, whereas the strip foundation placed at 'Mid' position is embedded in the slope face (Fig. 2).

To study the influence of effective column height of structure on the capacity of the foundation, a typical short pier bridge (with effective height = 5.0 m) and a typical RC building with storey height 3.0 m (having effective height = 1.5 m) have been considered (Fig. 1) and discussed in the following sections in detail. In addition, a two storey RC frame building having irregular ‘step-back’ configuration has been placed on face of the 20° slope and capacity envelopes of respective columns have been compared with the capacity envelopes of the supporting strip foundations, designed for various standards and literature.

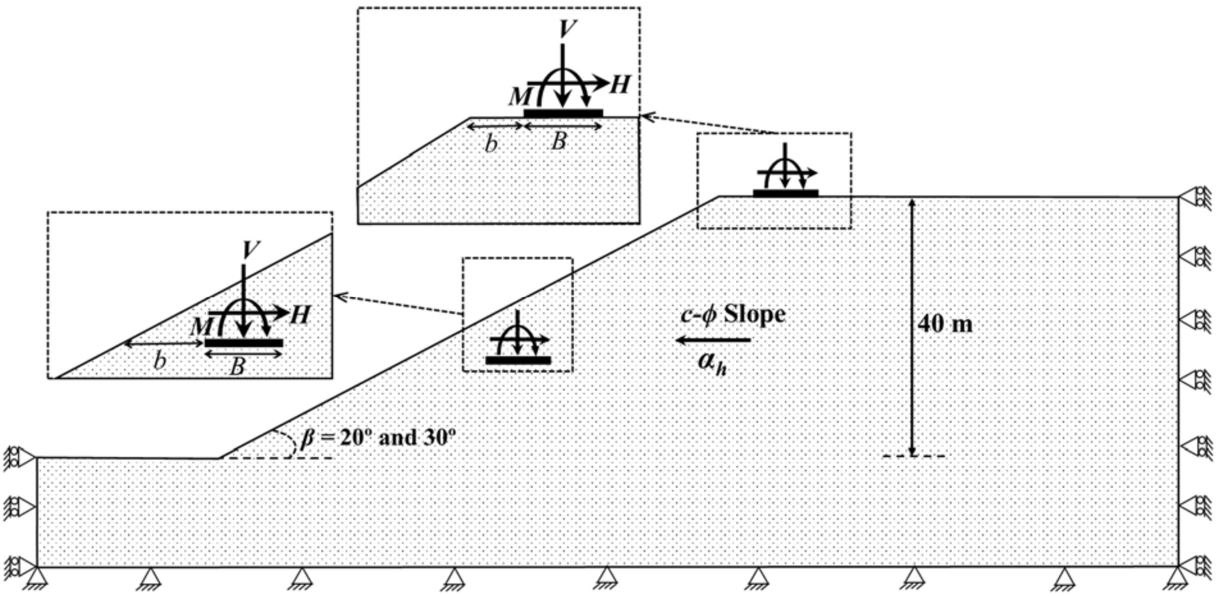


**Fig. 2.** Schematic diagram showing typical strip foundation under general planer loading located on slope

According to most seismic design codes, the pseudo-static analysis is performed using a fraction of the peak ground acceleration. For example, in IS1893-Part 1 (2016), the pseudo-static seismic load coefficient, $A_h$ (g) is dependent on the natural period of the structure, $T$, Seismic Zone Factor, $Z$ (representing the estimated effective peak ground acceleration, EPGA of the ground shaking), Response Reduction Factor, $R$ (reflecting the ductility capacity of the structure) and Importance Factor, $I$ (representing the acceptable damage level) of the structure, and is given as

$$A_h(g) = \frac{Z}{2}\frac{I}{R}S_a(T) \tag{1}$$

where, $S_a$ is the spectral acceleration corresponding to structural natural period $T$, normalized by EPGA. However, the seismic coefficient $\alpha_h$ representing the average peak acceleration of the soil mass, is usually adopted as half of effective peak ground acceleration (EPGA) at the ground surface (e.g. (EN1998-5 2004; NCHRP 2008). In the present study, the seismic coefficients for both slope and the building have been considered to be equal (i.e. $A_h = \alpha_h$). For a structure, base shear, $H$ and moment, $M$, is dependent on the seismic weight (= $V$) and effective height, $h$, of the structure as given by Eqns. 2 and 3.

$$H = \alpha_h V \tag{2}$$

$$M = Hh = \alpha_h h V \tag{3}$$

Table 1. Material properties

| Properties | Stiff Clay | Dense Sand |
|---|---|---|
| Unit Weight, $\gamma$ (kN/m$^3$) | 20 | 20 |
| Poisson's Ratio, $v$ | 0.3 | 0.3 |
| Cohesion, $c$ (kPa) | 50 | 10 |
| Angle of internal friction, $\phi$ | 27° | 44° |

**Modelling and Analysis**

FELA combines the capabilities of finite element discretization with the plastic bound theorems of limit analysis to bracket the exact limit load by upper and lower bound solutions for handling complex geometries, soil properties, loadings, and boundary conditions (Keawsawasvong and Ukritchon 2017). Application of limit analysis and FELA are extensively discussed by Chen and Liu (1990) and Sloan (2013) for analysing various complex stability problems in geotechnical engineering. The theorems of the limit analysis are valid for a perfectly plastic material with associated flow rule. In addition to LB and UB limit analysis, OptumG2 provides the option of 15-node triangular mixed element from Gauss family, where both the LB and UB problems under plane-strain condition are formulated using second-order cone programming (SOCP) (Makrodimopoulos and Martin 2006; Makrodimopoulos and

Martin 2007). The details of numerical formulation of FELA used in this study can be found in Krabbenhoft et al. (2016).

To understand the failure mechanism and to develop the capacity envelopes, 2D plane-strain nonlinear FE model of a slope with strip foundation has been constructed. An elasto-plastic constitutive model based on Mohr-Coulomb failure criterion with associated flow rule has been used for soil modeling in FELA. Because the focus is on the capacities, the Mohr-Coulomb model is satisfactory. In the present study, the soil mass has been discretized using triangular elements with 15-node mixed Gauss element formulation. The strip foundation has been modelled using plate element. The two-node elastic plate element in plane-strain domain actually acts like the standard Euler-Bernoulli beam element. The strip foundation has been considered as consisting of a rigid elastic material by using relatively large value of Young's modulus and has been embedded in the soil using interface elements on both sides of the foundation, such that the velocity and stress discontinuities are permitted. The interface properties have been simulated by applying a reduction factor, $R$ to the interface material properties. In the present study, the interface material has been considered the same as the surrounding soil but with zero tension cut-off to allow for gap and uplift and $R = 1$ to simulate rough foundation.

At the base of the FE model, the movements in both directions are restrained, while on the left and right lateral boundaries, only horizontal displacement is restrained. The lateral extent and dimensions of FE model have been evaluated using a sensitivity study, so that the effect of boundary conditions and model dimensions on the domain of interest is negligible. Automatic mesh adaptivity based on shear strain evolution has been employed. Based on a sensitivity and calibration test, five iterations of adaptive meshing with the number of elements increasing from 7000 to 10,000 have been used in all the analyses. To simulate the seismic effects on the coupled slope-foundation system, pseudo-static forces have been applied on the entire soil mass in terms of horizontal seismic coefficient, $\alpha_h$.

Force controlled 'swipe' and constant force-ratio 'probe' analyses were carried out to derive capacity envelopes of strip foundation under *V-M* and *V-H* load combinations. In both analyses, the forces and moment have been applied at the midpoint of the foundation. In the force controlled swipe test, the foundation was subjected to a vertical load *V* (varying between 0 and $V_0$ at an increment of $0.1V_0$) and gradually increasing moment till incipient material failure. The plot of the variation of the ultimate moment with *V*, provides the *V-M* capacity envelope. In constant force-ratio probe test, the foundation was subjected to vertical, *V* and horizontal, *H*, forces gradually increasing in a fixed ratio, till incipient material failure. The ratio *V*:*H* was varied between 1:0.05 and 1:1.10, in the successive steps, to obtain the *V-H* capacity envelope.

**Model Validation and Comparison with Past Studies**

To validate the adopted plane-strain FE model, normalized static *V-H* and *V-M* capacity envelopes for rigid rough strip foundation placed on surface of flat ground have been compared (Fig. 3(a-d)) with those obtained from available standards (EN1998-5 2004; NCHRP 2010) and past studies (Green 1954; Meyerhof 1963; Hansen 1970; Vesić 1975; Butterfield and Gottardi 1994; Paolucci and Pecker 1997; Ukritchon et al. 1998; Loukidis et al. 2008; Gourvenec and Barnett 2011; Tang et al. 2014). The forces (*V*, *H*) and moments (*M*) are normalized by $V_0$ and $BV_0$, respectively, where *B* is the width of the foundation and $V_0$ is the maximum static vertical load capacity of the foundation placed on flat ground in absence of *H* and *M*. The comparison was performed separately for dry cohesionless soil ($\phi$ = 38° and $\gamma$ = 20 kN/m$^3$) and dry cohesive soil ($c$ = 100 kPa and $\gamma$ = 20 kN/m$^3$).

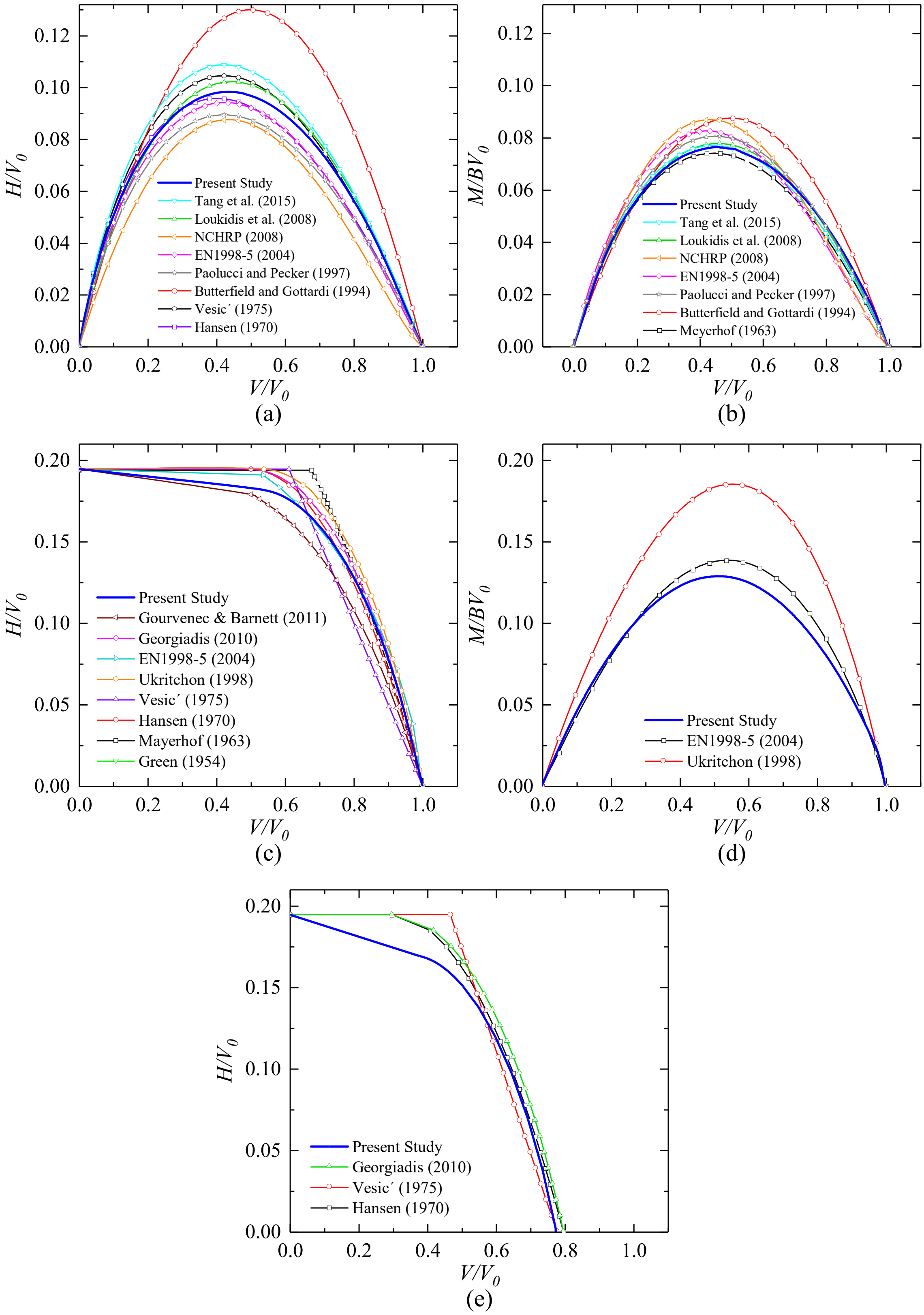


**Fig. 3.** Comparison of normalized capacity envelopes for rigid rough strip foundation obtained from the present study with those from the available standards/past studies: (a) *V-H* capacity envelope on flat cohesionless soil; (b) *V-M* capacity envelope on flat cohesionless soil; (c) *V-H* capacity envelope on flat cohesive soil; (d) *V-M* capacity envelope on flat cohesive soil; (e) *V-H* capacity envelope on a 30° slope of cohesive soil. (Here $V_0$ is the maximum vertical load capacity on flat ground, in absence of *H* and *M*)

It is to be noted that all these authors/codes have provided generalized normalized shapes of *V-M* and *V-H* capacity envelopes for cohesive and cohesionless soils. Further, Loukidis et al. (2008) have shown that the normalized shape of the capacity envelope is also independent of (associated/non associated) flow rule. In each case, the comparisons were made with as many of the considered studies and standards as possible. Figure 3 (a-e) presents the results of the comparisons and verifications.

It is evident from the figure that the present study predicts the capacity envelopes quite close to most of the considered standards/past studies, except Butterfield and Gottardi (1994), which overestimates the capacity for cohesionless soil in both *V-M* and *V-H* planes and Ukritchon et al. (1998) which overestimates the *V-M* capacity for cohesive soil. In addition, the *V-H* capacity envelope of a rough rigid foundation placed on top of a cohesive soil slope (slope height= 6 m, $\beta$ = 30°, $b/B$ = 0, $c$ = 100 kPa and $\gamma$ = 20 kN/m$^3$) has also been compared with the available literature (Hansen 1970; Vesić 1975; Georgiadis 2010) and found to be in good agreement (Fig. 3(e)).

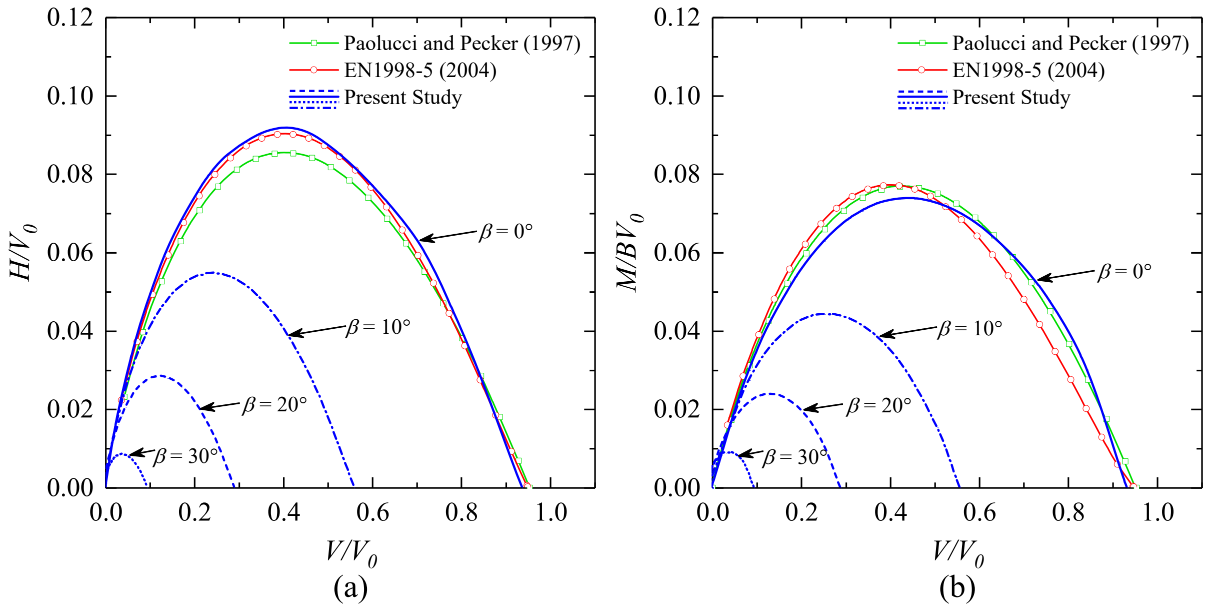


**Fig. 4.** Comparison of normalized capacity envelopes for rigid rough strip foundation (on cohesionless soil) obtained from the present study with those from the available standards/past studies: (a) *V-H* capacity envelope on flat ground and slopes of varying inclination, $\beta$; and (b) *V-M* capacity envelope on flat ground and slopes of varying inclination, $\beta$.

Among the available literature and codes, only Paolucci and Pecker (1997) and EN1998-5 (2004) consider the effect of earthquake on the capacity envelope. The results of the present study have also been compared (Fig. 4) with those of Paolucci and Pecker (1997) and EN1998-5 (2004) for a rough foundation on cohesionless soil ($\phi$ = 38° and $\gamma$ = 20 kN/m$^3$) subjected to $\alpha_h$ = 0.10 g. The results obtained using the present study by assuming the foundation to be located on slopes of different inclination ($\beta$ = 10°, 20° and 30°) have also been compared in the same plots. It should be noted that the available literature and codes do not provide capacity envelopes for foundations on slopes subjected to earthquake action. The comparison in Fig. 4 shows that the present study predicts the capacity envelopes quite close to those by Paolucci and Pecker (1997) and EN1998-5 (2004), also in presence of earthquake action. Further, the figure also illustrates the significance of seismic action in case of foundations located on slopes, and hence the relevance of the present study.

## Results and Discussion

Detailed investigation has been conducted to understand the influence of governing parameters such as $\alpha_h$, $b/B$ and effective column height of the structure, $h$ on the capacity envelope. Various failure patterns of the slope-foundation system have been identified in the different considered cases. The critical failure modes at different applied loads have also been identified comparing the $V$-$M$ and $V$-$H$ capacity envelopes. In the later part of the numerical study, the critical (governing) capacity envelopes of soil-foundation systems and supported columns, have been compared for a typical reinforced concrete (RC) building resting on a slope.

### Effect of seismic coefficient and offset distance

To study the effect of $\alpha_h$ and $b/B$ on the capacity, the normalized capacity envelope ($M/BV_0$ vs $V/V_0$ and $H/V_0$ vs $V/V_0$) are plotted for the 20° and 30° slopes and compared with their associated results for flat ground conditions. For the considered soil properties, the maximum (vertical) ultimate load, $V_0$ is equal to 3070 kN/m and 11607 kN/m for 'Stiff clay' and 'Dense sand', respectively. Normalized *V-M* and *V-H* diagrams for strip foundation placed on surface of flat ground, and on top and face of the 20° slope are presented in Figs. 5(a, b), 5(c, d) and 5(e, f), respectively. Similarly, Figs. 6(a, b), 6(c, d) and 6(e, f), present the normalized *V-M* and *V-H* diagrams for strip foundation located on flat ground, and top and face of the 30° slope, respectively. It is evident from Figs. 5(a, b) and Figs. 6(a, b) that the *V-M* and *V-H* capacity envelopes on flat ground, are not much influenced by the variation in $\alpha_h$. On the other hand, in case of foundations on slopes, the *V-M* and *V-H* capacity envelopes of the seismic case, become gradually reduced subsets of the respective static case ($\alpha_h$ = 0), with increase in $\alpha_h$ for a particular *b/B,* as can be observed from Figs. 5(c-f) and Figs. 6(c-f). It can also be observed that for a particular $\alpha_h$, the *V-M* and *V-H* capacity envelopes of a strip foundation with *b/B* > 0 fully encompass the corresponding envelopes of the strip foundation placed at *b/B* = 0, in all the cases.

It can be observed from Figs. 5(c-f) and 6(c-f) that for a particular vertical load, the moment and shear capacities of the foundation towards and away from the slope are significantly different, resulting in asymmetrical *V-M* and *V-H* capacity envelopes. However, the degree of asymmetry in *V-H* envelopes is much more significant and increases with the increase in $\alpha_h$ (see Figs. 5(d and f) and 6(d and f)). It is interesting to note that a much higher vertical load (in some cases, even higher than the maximum vertical load capacity in case of flat ground) can be resisted by the foundation on slope, when combined with appropriate value of shear force in the positive (uphill) direction. Further, not one but two values of positive shear force, yield the same vertical load capacity.

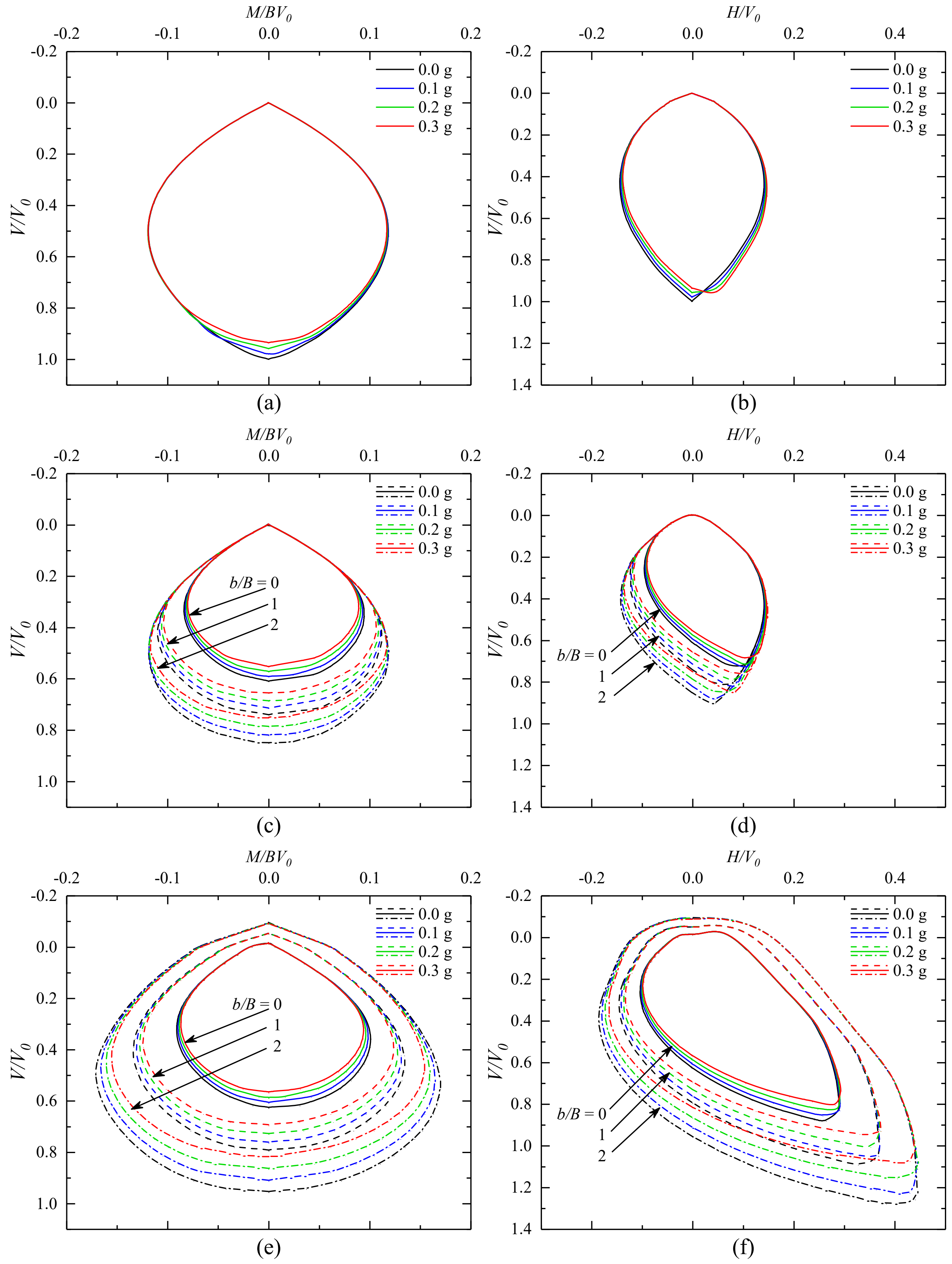


**Fig. 5.** Capacity envelopes for foundations on flat and sloping ground having 'Stiff clay' properties: (a) *V-M* capacity curves on flat ground; (b) *V-H* capacity curves on flat ground; (c) *V-M* capacity curves on top of 20° slope; (d) *V-H* capacity curves on top of 20° slope; (e) *V-M* capacity curves on face of 20° slope; and (f) *V-H* capacity curves on face of 20° slope.

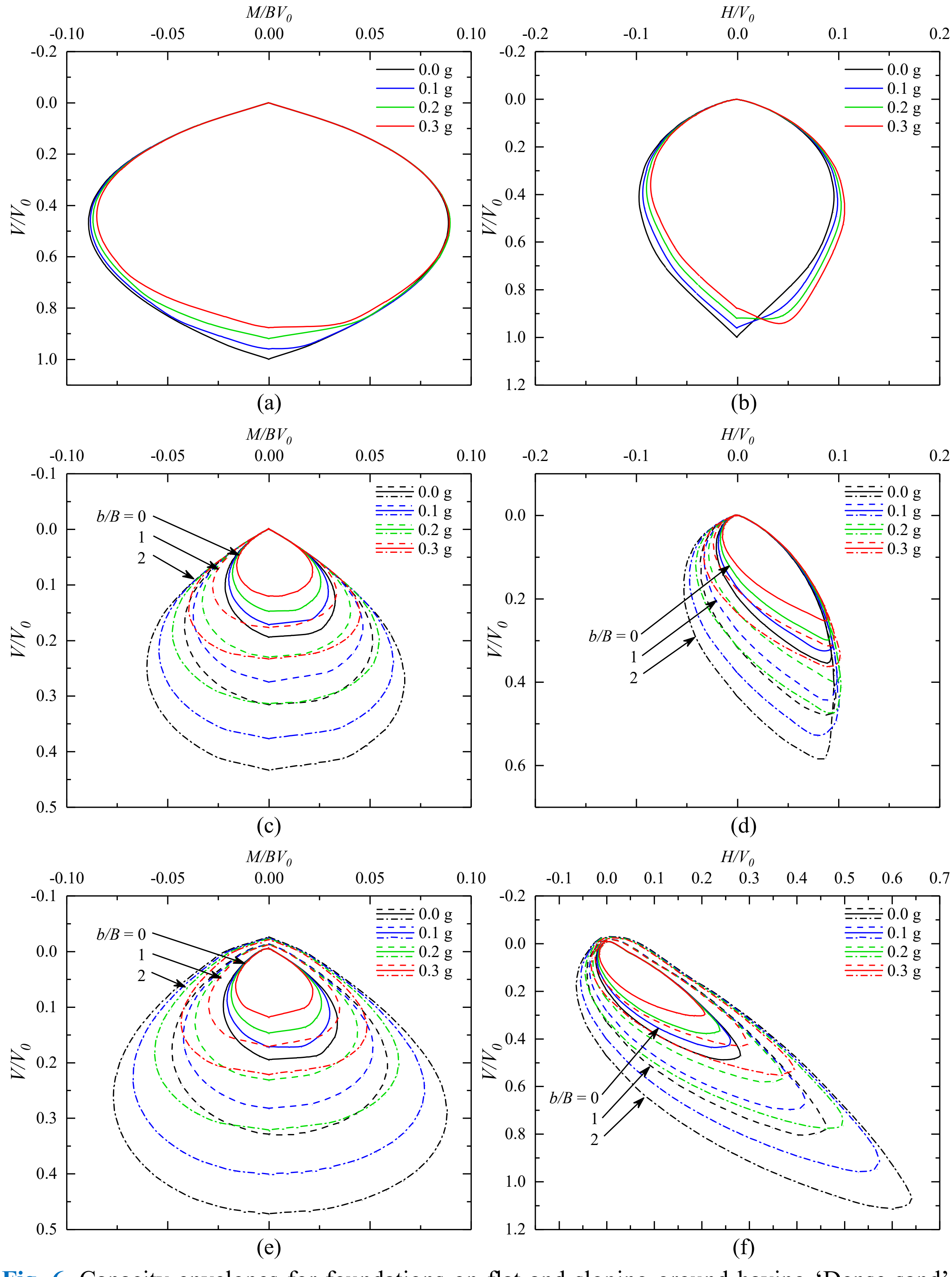


**Fig. 6.** Capacity envelopes for foundations on flat and sloping ground having 'Dense sand' properties: (a) *V-M* capacity curves on flat ground; (b) *V-H* capacity curves on flat ground; (c) *V-M* capacity curves on top of 30° slope; (d) *V-H* capacity curves on top of 30° slope; (e) *V-M* capacity curves on face of 30° slope; and (f) *V-H* capacity curves on face of 30° slope.

Table 2. Percentage change in maximum vertical, shear and moment capacities of strip foundation located slope, in comparison with the flat ground

| $b/B$ | $\alpha_h$ | Top of 20° slope | | | | | Face of 20° slope | | | | | Top of 30° slope | | | | | Face of 30° slope | | | | |
|---|---|---|---|---|---|---|---|---|---|---|---|---|---|---|---|---|---|---|---|---|---|
| | (g) | $V_m$ | $M_m^-$ | $M_m^+$ | $H_m^-$ | $H_m^+$ | $V_m$ | $M_m^-$ | $M_m^+$ | $H_m^-$ | $H_m^+$ | $V_m$ | $M_m^-$ | $M_m^+$ | $H_m^-$ | $H_m^+$ | $V_m$ | $M_m^-$ | $M_m^+$ | $H_m^-$ | $H_m^+$ |
| 0 | 0 | -39 | -30 | -20 | -34 | 0 | -37 | -24 | -15 | -28 | 105 | -81 | -76 | -63 | -79 | -1 | -80 | -75 | -62 | -78 | 198 |
| | 0.1 | -41 | -31 | -22 | -35 | 2 | -39 | -25 | -17 | -29 | 105 | -83 | -78 | -67 | -81 | 0 | -83 | -77 | -66 | -81 | 175 |
| | 0.2 | -43 | -32 | -23 | -36 | 3 | -41 | -26 | -19 | -30 | 106 | -85 | -80 | -71 | -83 | -3 | -85 | -79 | -71 | -83 | 152 |
| | 0.3 | -45 | -33 | -25 | -38 | 4 | -43 | -27 | -21 | -32 | 107 | -88 | -82 | -75 | -86 | -7 | -88 | -82 | -75 | -86 | 119 |
| 1 | 0 | -26 | -7 | -5 | -13 | 0 | -20 | 12 | 13 | 2 | 159 | -68 | -53 | -42 | -62 | 1 | -67 | -46 | -34 | -58 | 389 |
| | 0.1 | -28 | -9 | -7 | -15 | 2 | -24 | 10 | 10 | -1 | 161 | -72 | -58 | -47 | -66 | 5 | -72 | -52 | -42 | -64 | 338 |
| | 0.2 | -31 | -11 | -8 | -17 | 3 | -27 | 7 | 7 | -4 | 162 | -77 | -63 | -54 | -71 | 5 | -77 | -59 | -50 | -70 | 291 |
| | 0.3 | -34 | -13 | -10 | -19 | 4 | -30 | 4 | 4 | -7 | 162 | -82 | -69 | -62 | -76 | 0 | -83 | -67 | -60 | -77 | 214 |
| 2 | 0 | -15 | 0 | 0 | -2 | 0 | -4 | 44 | 43 | 30 | 213 | -57 | -32 | -24 | -45 | 1 | -53 | -13 | 0 | -35 | 577 |
| | 0.1 | -18 | 0 | 0 | -3 | 2 | -9 | 40 | 39 | 26 | 213 | -62 | -39 | -30 | -51 | 5 | -60 | -24 | -13 | -44 | 499 |
| | 0.2 | -21 | -1 | -1 | -4 | 3 | -13 | 35 | 35 | 21 | 213 | -69 | -46 | -38 | -58 | 9 | -68 | -37 | -27 | -55 | 424 |
| | 0.3 | -25 | -2 | -2 | -6 | 4 | -18 | 35 | 35 | 17 | 210 | -77 | -56 | -49 | -66 | 8 | -78 | -51 | -45 | -67 | 317 |

*Note: $V_m$ = Maximum vertical load capacity; $M_m^-$ = Maximum moment capacity in negative direction; $M_m^+$ = Maximum moment capacity in positive direction; $H_m^-$ = Maximum shear capacity in negative direction and $H_m^+$ = Maximum shear capacity in positive direction.

Table 2 presents the percentage variation in maximum vertical load capacity, $V_m$ (in absence of $M$ and $H$), maximum moment capacity, $M_m$ and maximum shear capacity, $H_m$ of strip foundation located on top and face of 20° and 30° slopes at different $b/B$, in comparison with the respective capacities of the surface strip foundation on flat ground. It can be observed from the table that $V_m$ and $M_m$ reduce by around 35-45% and 15-30%, respectively for the 20° slope. Whereas, in case of the 30° slope the corresponding reductions are around 80-90% and 60-80%, respectively. In case of the maximum shear force, $H_m$ there is a reduction of about 30-40% in the negative direction and an increase of about 100-200% in the positive direction for 20° slope. In case of the 30° slope the corresponding decrease and increase are as high as about 80-90% and 0-600%, respectively. These results indicate that in case of foundations on slopes, not only the capacity envelopes are asymmetric, the influence of $\alpha_h$ and $b/B$ is also asymmetric, resulting in increasingly asymmetric capacity envelopes.

**Failure patterns**

Figures 7 and 8 show the failure mechanisms for different combinations of vertical load with moment and shear, marked on the normalized $V$-$M$ and $V$-$H$ capacity envelopes, respectively. The failure mechanisms are shown for strip foundations embedded at $b/B$ =1 on face of 20° slope and subjected to a seismic coefficient, $\alpha_h$ = 0.2g. Similar observations have also been made in all other considered cases (not shown here for brevity).

It can also be observed from the figures that the failure mechanism changes continuously with the vertical load. In case of the maximum vertical load (without $H$ and $M$), the bearing failure with a triangular wedge below the full width of the foundation, takes place. It is similar to the bearing failure on flat ground, except that the failure in case of sloping ground is asymetric and shear wedge forms only in the downhill direction. For the upward (negative) vertical load, a trapezoidal shear wedge is formed providing some capacity against foundation uplift. Under the negative moment, a triangular vedge forms under the compression edge of the footing and the width of the triangular wedge increases gradually with the increasing vertical load. However, for positive moment, formation of triangular wedge beneath the foundation is not observed.

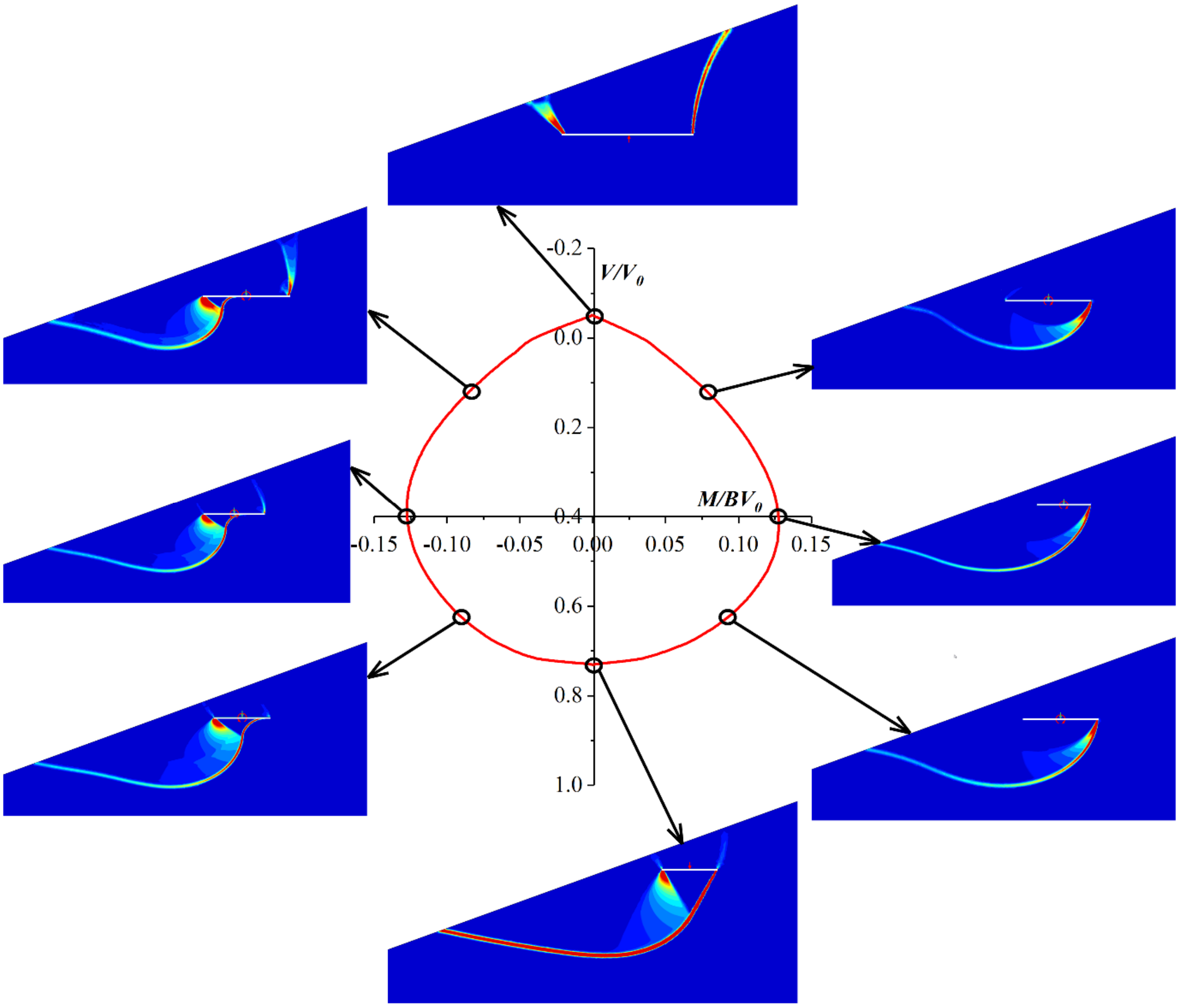


**Fig. 7.** Failure patterns for $V$-$M$ load interaction for $\alpha_h = 0.2$g

Under the combined action of vertical and shear loads, the triangular wedge forms for both directions of the applied shear force. However, the shear failure takes place asymmetrically only in one direction, with shear wedge forming either in uphill or in downhill direction. Interestingly, the change in the direction of the shear wedge failure takes place at the lower vortex (representing the maximum vertical load the foundation can resist in *V-H* intercation, which is higher than the maximum pure vertical load capacity without moment and shear) of the *V-H* interaction curve. This explains the possibility of two values of shear capacities in posive direction, for a given value of vertical load. Under the combination of the vertical load with the lower value of shear capacity, the failure occurs in downhill direction, whereas in case of the higher value of the shear capacity, the failure occurs in uphill direction.

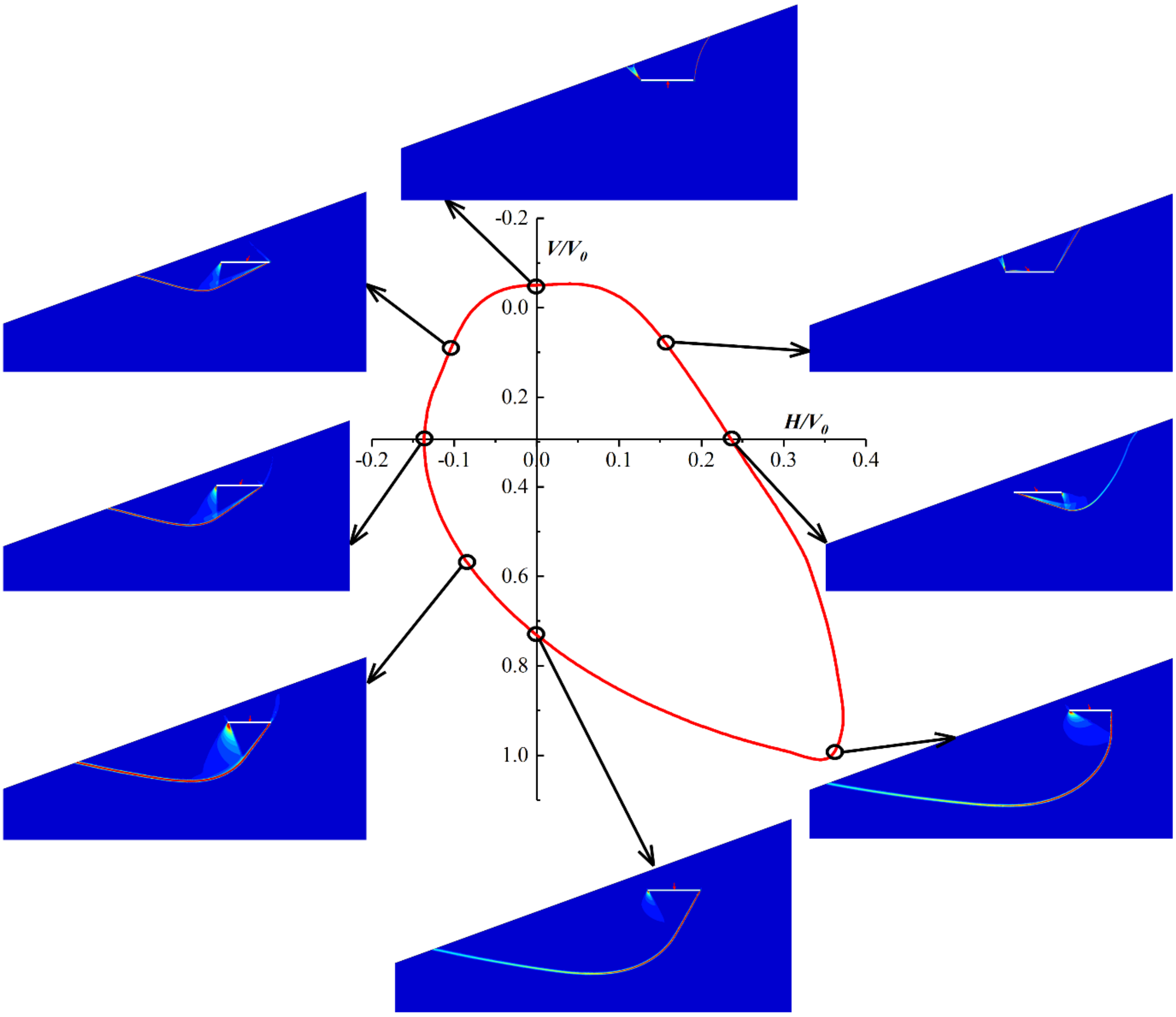


**Fig. 8.** Failure patterns for *V-H* load interaction for $\alpha_h$ = 0.2g

**Relative influence of soil and structure inertia**

Figures 9(a-c) and Figs. 9(d-f) reproduce (from Figures 5 and 6) the normalized *V-M* capacity envelopes for the strip foundation placed on surface of flat ground and on top and face (at *b/B* = 0) of 20° and 30° slopes, respectively, subjected to varying seismic coefficient. In these figures, inclined straight lines with slope representing the quantity, $\alpha_h h/B$ are added. The different colours of the firm-line curves represent the effect of varying soil inertia force on the *V-M* capacity envelope, whereas the different coloured dashed lines represent the effect of structure inertia and effective height. Further, the intersection points of the black (vertical) dashed line and capacity envelopes of different colours, represent the maximum vertical load capacity considering the effect of the soil mass inertia only, whereas the intersection point of a coloured (inclined) dashed line with the capacity envelope of the same colour in either direction, indicates the maximum vertical load capacity considering the combined effect of the soil mass inertia and effective structure height. Similarly, Figs. 10(a-c) and Figs. 10(d-f) reproduce (from Figures 5 and 6) the normalized *V-H* capacity envelopes for strip foundations placed on surface of flat ground, and on top and face (at *b/B* = 0) of 20° and 30° slopes, respectively. In this case, the slope of the inclined dashed lines of different colours represent the effect of structure inertia in terms of the seismic coefficient, $\alpha_h$.

It can be observed from Figs. 9 and 10 that the effect of soil inertia on capacity of strip foundations resting on the flat ground is only marginal, whereas in case of sloping ground, this effect is quite significant and even more pronounced in case of the 30° slope. On the other hand, the effect of structure's inertia and effective height is significant in all the cases. The figures also illustrate the asymmetric effect of soil and structure inertia due to seismic excitation towards and away from the slope.

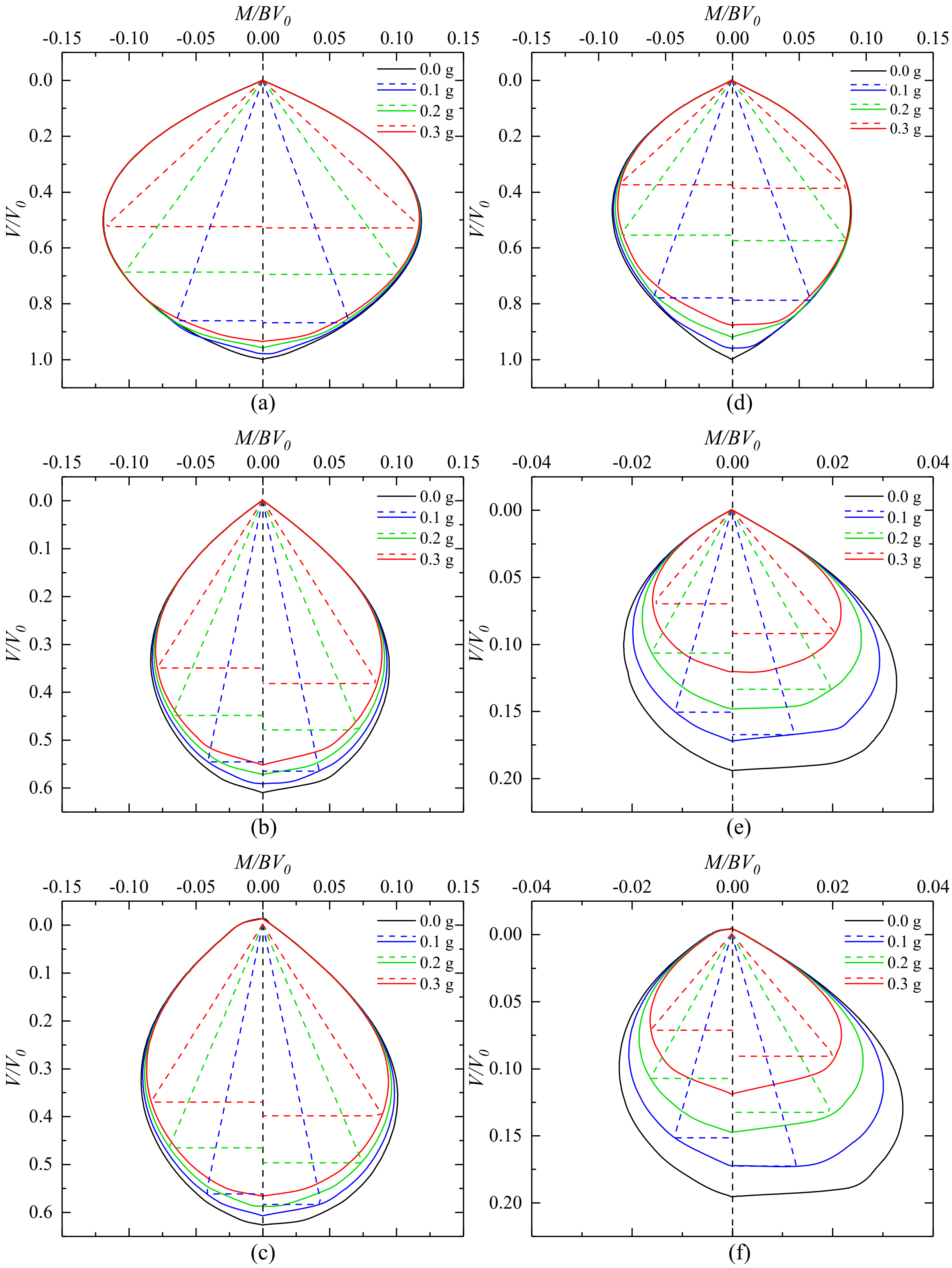


**Fig. 9.** *V-M* capacity envelopes for foundations placed on: (a) flat ground having 'Stiff clay' properties; (b) top of 20° slope; (c) face of 20° slope; (d) flat ground having 'Dense sand' properties; (e) top of 30° slope; and (f) face of 30° slope. (Inclined dashed lines show different $\alpha_h h/B$ for $h$ = 1.5 m and $B$ =2.0 m)

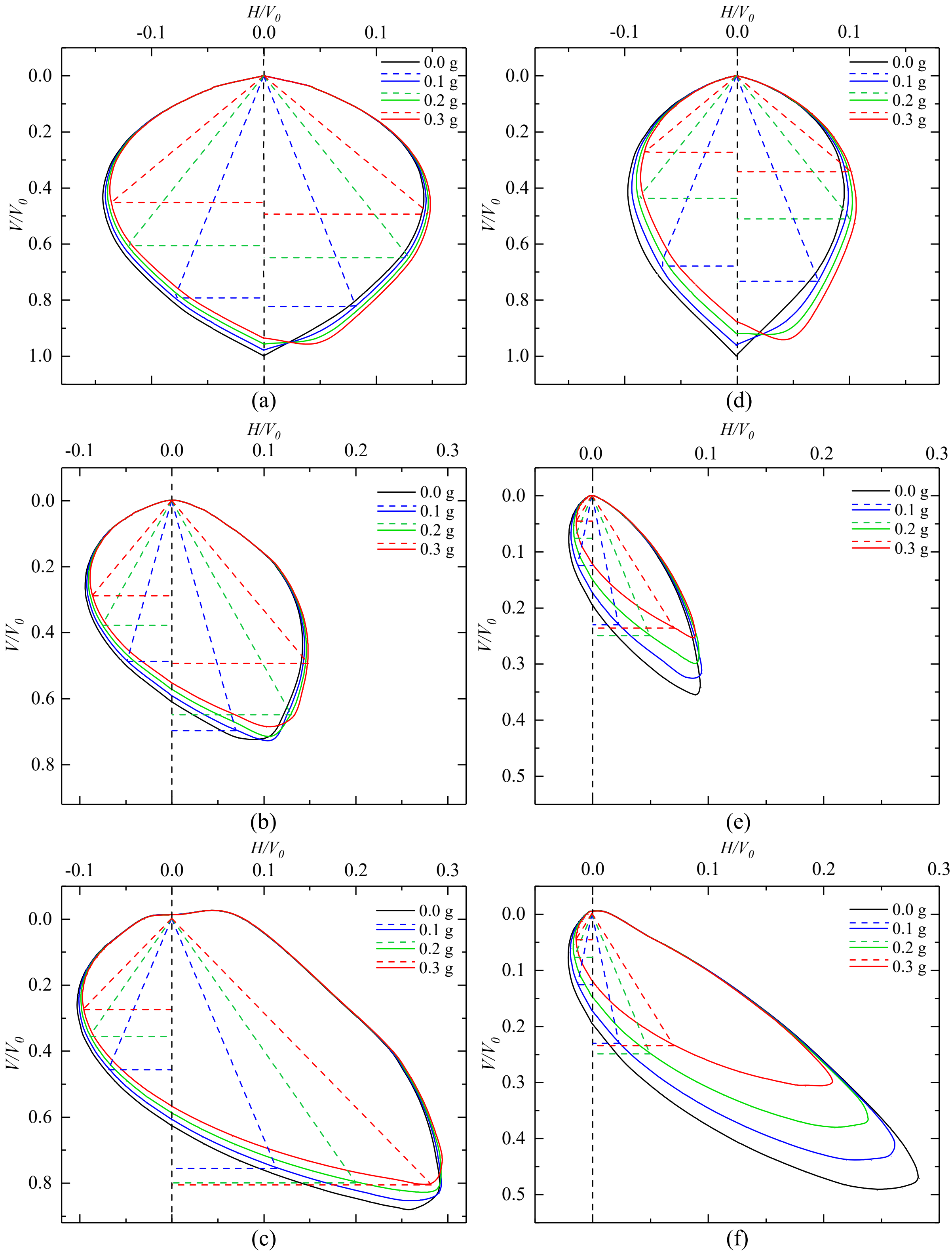


**Fig. 10.** *V-H* capacity envelopes for foundations placed on: (a) flat ground having 'Stiff clay' properties; (b) top of 20° slope; (c) face of 20° slope; (d) flat ground having 'Dense sand' properties; (e) top of 30° slope; and (f) face of 30° slope.

**Critical failure mode and governing capacity envelope**

To identify the critical failure mode, the *V-M* capacity envelopes have been compared (Fig. 11) with the corresponding *V-H* capacity for a strip foundation located on surface of flat ground, and on top and face (at *b/B* =0) of 20° slope subjected to $\alpha_h$ = 0.20g. To facilitate direct comparison, the shear capacity has also been expressed in terms of equivalent moment, by multiplying with effective height. Figures 11(a-c) show the capacity envelopes for *h* = 1.5 m, representing a typical building with storey height = 3 m, whereas Figures 11(d-f) show the capacity envelopes for *h* = 5 m, representing a short pier bridge. Similarly, Fig. 12 shows the comparison of the capacity envelopes for the 30° slope. The red coloured curves in the figures, indicate the moment capacity and the blue coloured curves indicate the shear capacity.

It can be observed from Figs. 11 (a-c) and 12(a-c) that in the positive direction, the failure is governed by the moment capacity, for both the slopes and both the effective heights, whereas, in the negative direction, the failure of the strip foundation depends on *V* and *h*. In case of shorter structures (*h* = 1.5 m), the failure is governed by shear capacity for lower values of *V*, whereas in case of taller structures (*h* = 5 m) and for higher values of *V*, even in case of shorter structures, the failure is governed by the moment capacity.

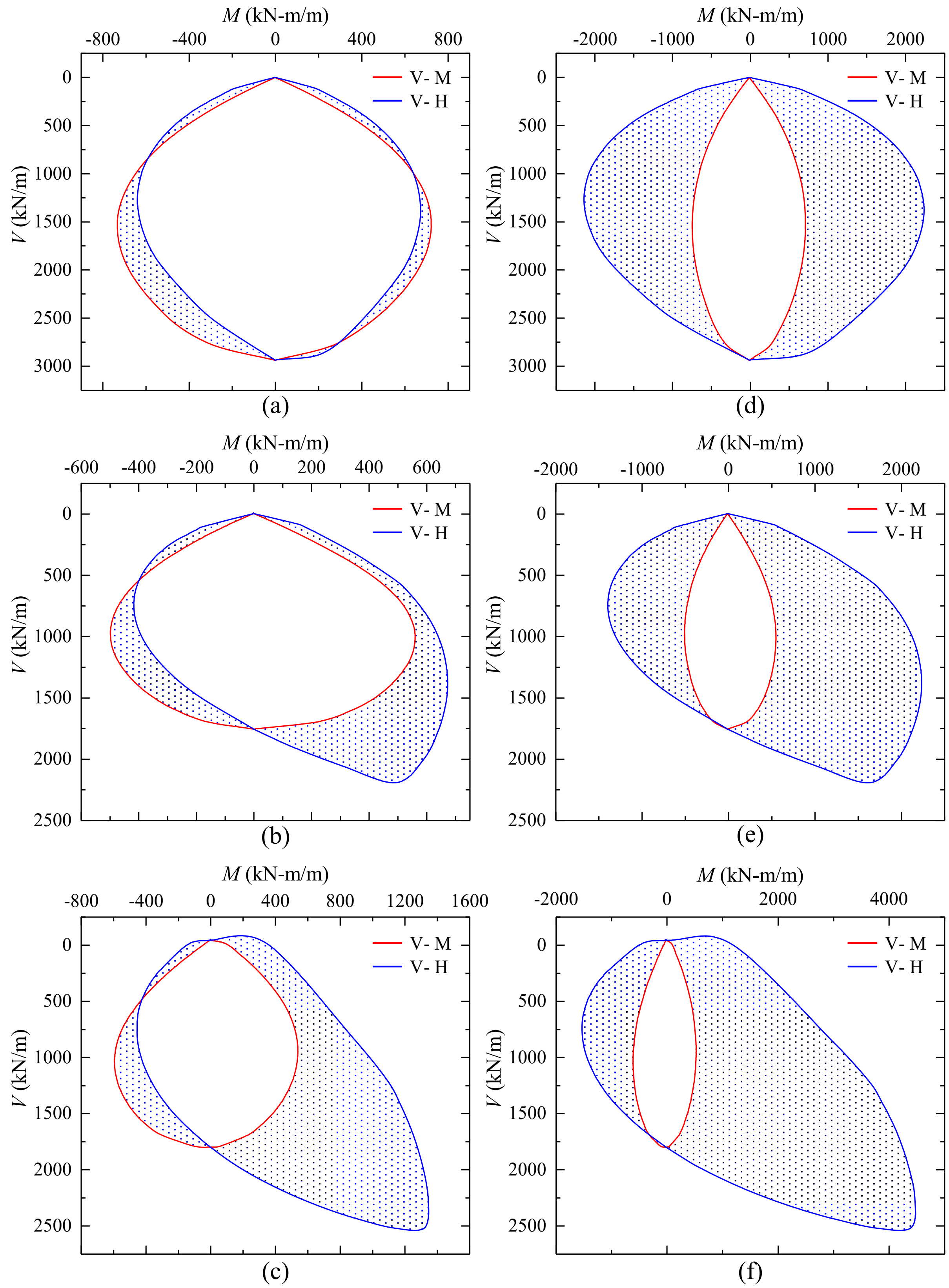


**Fig. 11.** Combined *V-H* and *V-M* capacity envelopes for foundations placed on: (a) flat ground having 'Stiff clay' properties, $h$ = 1.5 m; (b) top of 20° slope, $h$ = 1.5 m; (c) face of 20° slope, $h$ = 1.5 m; (d) flat ground having 'Stiff clay' properties, $h$ = 5 m; (e) top of 20° slope, $h$ = 5 m; and (f) face of 20° slope, $h$ = 5 m.

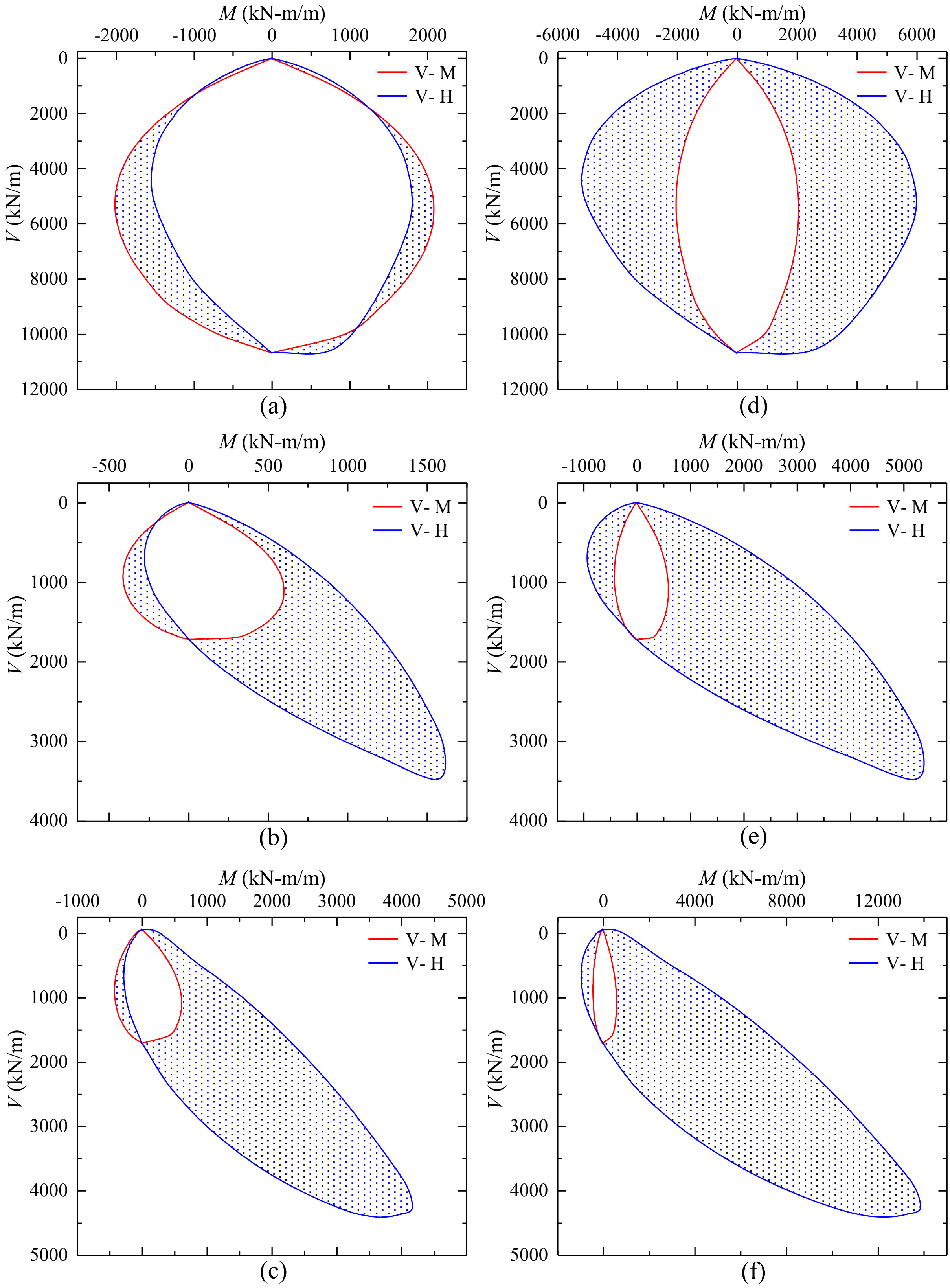


**Fig. 12.** Combined *V-H* and *V-M* capacity envelopes for foundations placed on: (a) flat ground having ‘Dense sand’ properties, $h = 1.5$ m; (b) top of 30° slope, $h = 1.5$ m; (c) face of 30° slope, $h = 1.5$ m; (d) flat ground having ‘Dense sand’ properties, $h = 5$ m; (e) top of 30° slope, $h = 5$ m; and (f) face of 30° slope, $h = 5$ m.

**Comparison of column and foundation capacities**

In performance based seismic design (PBSD), performance of a structure depends heavily on the sequence of yielding, which in-turn depends on the hierarchy of strength, of individual structural components (i.e. columns, beams and walls). The foundations are generally assumed to be stiffer and stronger than the columns supported on them, resulting in yielding taking place in columns. However, it may not always be true, especially in case of foundations located on slopes. In this section, capacity envelopes of foundations of a typical reinforced concrete (RC) frame building located on a slope are compared with the capacity envelopes of the corresponding RC columns. A two storey building having irregular ‘step-back’ configuration to suit the slope geometry, has been considered to be located on the face of the 20° slope. Figure 13 (a-b) shows the plan and elevations of the RC frame building considered in this study.

In the 2D model, one single frame (Frame ‘B’) of the building has been modeled with the corresponding tributary loads on beams and columns as shown in the Fig. 13. The lateral force acting on the building has been considered corresponding to the lateral seismic coefficient, $\alpha_h$ = 0.12g, representing the Seismic Zone IV of IS1893-Part 1 (2016), using the dynamic mode superposition method. This method, recommended by most of the current seismic design codes, considers the effect of inelastic energy dissipation on the actual force transmitted to the foundation-soil system, indirectly using a response reduction factor (or behaviour factor). To find out the lateral forces acting on the building, due to earthquake, first the building has been modelled with fixed-base condition in SAP2000 (2018) structural analysis and design software, and mode superposition analysis has been performed. The structural elements (beams and columns) have been assigned the properties of M30 grade concrete (unit weight, $\gamma$ = 25 kN/m$^3$; Poisson’s ratio, $v$ = 0.20; and Young’s modulus, $E$ = 27 GPa) and Fe500 grade steel (unit weight, $\gamma$ = 78.5 kN/m$^3$; Poisson’s ratio, $v$ = 0.30; and Young’s modulus, $E$ = 200 GPa). The beam sizes are considered as 0.23 m × 0.40 m and the column sizes as 0.40 m × 0.40 m throughout the height. These dimensions are typical and based on a precise design using Indian codes (IS456 2000; IS1893 2016; IS13920 2016).

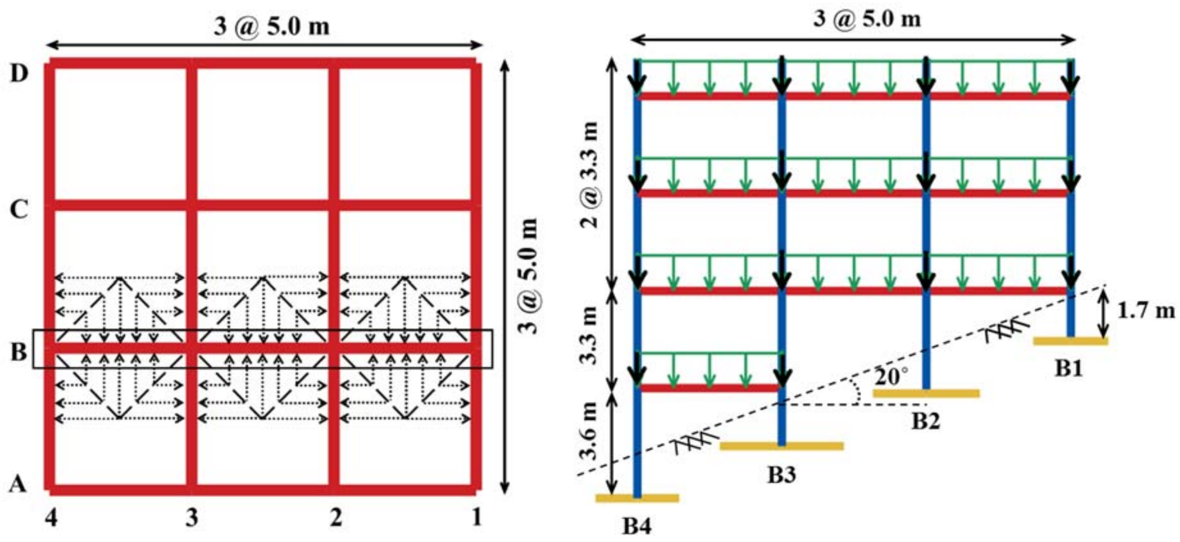


(a) (b)

**Fig. 13.** Plan and elevation of the considered building on the 20° slope: (a) plan showing tributary load on a typical frame 'B'; and (b) elevation of the typical frame.

The foundations of the building have been designed as strip foundations embedded to an average depth of 1.5 m below the soil surface. All foundations have been designed with a factor of safety equal to 3, using various standards (IS6403 1986; EN1997-1 2004) and literature Raj et al. (2018) (EN1998-5 (2004) and NCHRP (2008) could not be used as these provide capacity envelopes either for purely cohesive or purely frictional soils). The standards (IS6403 1986; EN1997-1 2004) provide guidelines for estimating the static bearing capacity of foundations located on flat ground, whereas Raj et al. (2018) have provided design aids for considering the effect of slope angle and seismic load (equal $\alpha_h$ on soil and structure) on bearing capacity of foundation. Table 3 shows the design forces and the estimated widths of the foundations. While using the Raj et al. (2018) method for design for foundation B4, the shear forces and monents on the foundation, being very small, have been ignored.

Table 3. Foundation dimension

| Foundation | Design Forces | | | Foundation Width (m) | | |
|---|---|---|---|---|---|---|
| | $V$ (kN/m) | $H$ (kN/m) | $M$ (kN-m/m) | IS6403 (1986) | EN1997-1 (2004) | Raj et al. (2018) |
| B1 | 490 | 164 | 229 | 2.4 | 3.0 | 4.6 |
| B4 | 842 | 13 | 25 | 1.2 | 1.6 | 2.2 |

Figure 14 shows the capacity envelopes of foundation B1 (supporting the 'short' uppermost column) and B4 (supporting a 'regular' column) compared with the capacity curves of the corresponding columns. It is to be noted that the foundation B1 is subjected to larger shear force and bending moment whereas foundation B4 is subjected to larger vertical load. It is due to the distribution of lateral force in different columns of a frame building in proportion to their stiffness, while the vertical force is distributed largely in proportion to the tributary floor areas of different columns. In the figure, the shear capacity of the foundation has also been shown as equivalent moment (by multiplying with effective height of the column bending in double curvature) to allow direct comparison. The shear capacity envelopes for the columns are not shown here, as the capacity design of columns, which is a common practice in all the building codes for design of RC columns, eliminates column failure in shear.

A comparison of the maximum vertical load capacity of the column and foundation can be misleading, as the vertical load on a column has relatively smaller change during earthquake, in comparison with the shear force and bending moment. Therefore, a more realistic indicator of the sequence of failure is comparison of shear and moment capacities at the usual vertical load. The peak axial force in the column under combined action of gravity and earthquake, which is also equal to the vertical load on the corresponding foundation, is shown in the figure by dashed horizontal lines. The moment and shear capacities of the columns and the foundations can be compared at this vertical load.

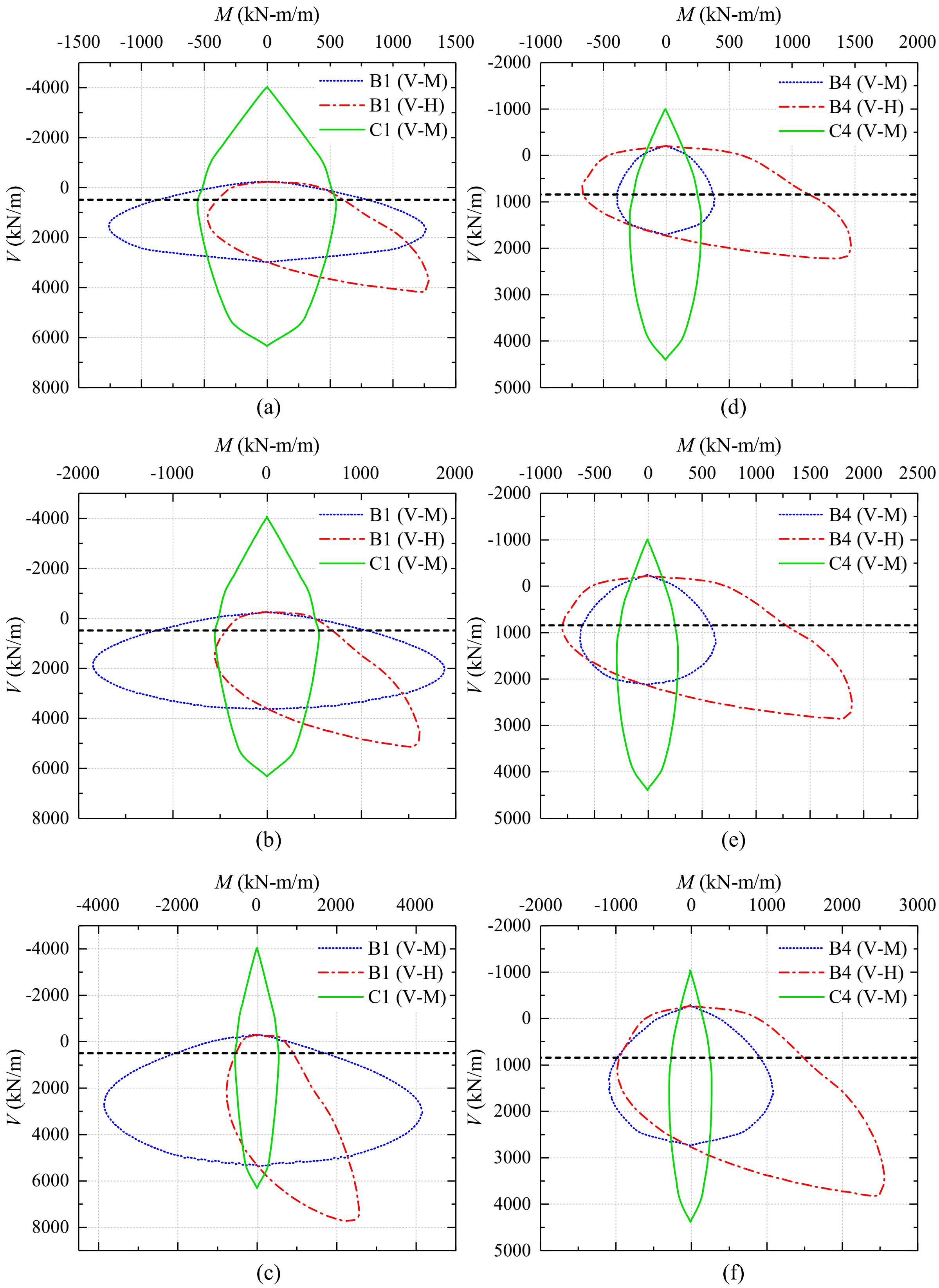


**Fig. 14.** Comparison of interactive capcity envelopes for columns and foundations: (a) foundation B1 designed using IS6403 (1986); (b) foundation B1 designed using EN1997-1 (2004); (c) foundation B1 designed using Raj et al. (2018); (d) foundation B4 designed using IS6403 (1986); (e) foundation B4 designed using EN1997-1 (2004); and (f) foundation B4 designed using Raj et al. (2018).

Figure 14 shows that while moment capacity of the foundations is higher than the capacity of the corresponding columns, in all the considered cases, the shear capacity of foundation B1 designed as per IS6403 (1986) and EN1997-1 (2004) is much lower than the capacity of the corresponding column. This indicates that during a strong seismic event, the foundation will fail in shear prior to flexural yielding of the column. Interestingly, the shear capacity of foundation B1 designed as per Raj et al. (2018) is close to the capacity of the corresponding column. However, this closeness is also coincidental, as the design using this method does take into account the effect of slope and shear due to $\alpha_h$, but the design methodology for RC members and foundations being different, results in different amounts of over-strength (reserve strength).

## Conclusions

A numerical study has been performed to understand the behaviour and failure modes of strip foundation placed at different locations on stable slopes, subjected to seismic loading including inertial effect of soil mass. The behaviour and capacity envelopes of strip foundations placed on slopes, under general planar loading, have been compared with their counterpart soil-foundation systems on flat ground. Contrary to the symmetric failure mechanism of strip foundations on flat ground, distinctly different failure mechanisms have been observed for the strip foundations placed on the slopes under different directions of seismic excitation. This effect is also reflected by the asymmetry in the *V-M* and *V-H* capacity envelopes and is more prominent with increasing slope angles. It is interesting to note that the foundations on slope can resist higher vertical loads when applied in combination with appropriate magnitude of shear force acting in positive (towards slope) direction. Further, for this vertical load ($> V_m$) there exist two values of positive shear corresponding to two different failure modes.

The study has clearly brought out the two different effects (i.e. due to soil inertia and due to structure inertia) of earthquake action, on foundation capacity. In case of the flat ground and moderate (20°) slope, the effect of soil inertia is only marginal but the effect of structure inertia is quite significant, whereas in case of steeper (30°) slope, both the effects are quite significant.

The shear capacity of foundations on slopes, in positive direction, being much higher, the failure is invariably governed by moment. However in case of negative direction, the effective height of the structure and amount of vertical load govern the failure mode.

A comparison of the capacity envelopes of the foundations and corresponding RC columns indicates that the conventionally designed foundations (without considering the effects of slope and soil and structure inertia forces, on the bearing capacity) are expected to fail before yielding of the RC columns. This is contrary to the commonly used philosophy of capacity design, in which the plastic hinges are assumed to form in the superstructure.

**Acknowledgments**

The research work presented here was supported by the Institute fellowship to the first author from the Ministry of Human Resource Development, Government of India. The authors are grateful to 'Optum Computational Engineering' (OptumCE) for providing free academic license of OptumG2 software to perform the present study.

**References**

ASCE/SEI41-13 (2014). "Seismic Evaluation and Retrofit of Existing Buildings." American Society of Civil Engineers, Reston, Virginia.

Baazouzi, M., Benmeddour, D., Mabrouki, A., and Mellas, M. (2016). "2D Numerical Analysis of Shallow Foundation Rested Near Slope under Inclined Loading." *Procedia Engineering*, 143, 623-634.

Bransby, M. F. (2001). "Failure envelopes and plastic potentials for eccentrically loaded surface footings on undrained soil." *International Journal for Numerical and Analytical Methods in Geomechanics*, 25(4), 329-346.

Butterfield, R., and Gottardi, G. (1994). "A complete three-dimensional failure envelope for shallow footings on sand." *Géotechnique*, 44(1), 181-184.

Butterfield, R., and Gottardi, G. (1994). "Plastic response of circular footings on sand under general planar loading." *Géotechnique*, 44(1), 181-184.

Butterfield, R., Houlsby, G. T., and Gottardi, G. (1997). "Standardized sign conventions and notation for generally loaded foundations." *Géotechnique*, 47(5), 1051-1054.

Chen, W. F., and Liu, X. L. (1990). *Limit analysis in soil mechanics*, Elsevier, Amsterdam.

Cocjin, M., and Kusakabe, O. (2013). "Centrifuge observations on combined loading of a strip footing on dense sand." *Géotechnique*, 63(5), 427-433.

EN1997-1 (2004). "Eurocode 7: Geotechnical design - Part 1: General rules." British Standards Institution, London.

EN1998-5 (2004). "Design Provisions for Earthquake Resistance of Structures- Part 5: Foundations, retaining structures and geotechnical aspects." British Standards Institution, London.

Fotopoulou, S. D., and Pitilakis, K. D. (2013). "Fragility curves for reinforced concrete buildings to seismically triggered slow-moving slides." *Soil Dynamics and Earthquake Engineering*, 48, 143-161.

Georgiadis, K. (2010). "The influence of load inclination on the undrained bearing capacity of strip footings on slopes." *Computers and Geotechnics*, 37(3), 311-322.

Gottardi, G., and Butterfield, R. O. Y. (1993). "On the bearing capacity of surface footings on sand under general planar loads." *Soils and Foundations*, 33(3), 68-79.

Gottardi, G., and Butterfield, R. O. Y. (1995). "The displacement of a model rigid surface footing on dense sand under general planar loading." *Soils and Foundations*, 35(3), 71-82.

Gottardi, G., Houlsby, G. T., and Butterfield, R. (1999). "Plastic response of circular footings on sand under general planar loading." *Géotechnique*, 49(4), 453-469.

Gourvenec, S. (2007a). "Shape effects on the capacity of rectangular footings under general loading." *Géotechnique*, 57(8), 637-646.

Gourvenec, S. (2008). "Effect of embedment on the undrained capacity of shallow foundations under general loading." *Géotechnique*, 58(3), 177-185.

Gourvenec, S., and Barnett, S. (2011). "Undrained failure envelope for skirted foundations under general loading." *Géotechnique*, 61(3), 263-270.

Gourvenec, S., and Randolph, M. (2003). "Effect of strength non-homogeneity on the shape of failure envelopes for combined loading of strip and circular foundations on clay." *Géotechnique*, 53(6), 575-586.

Govoni, L., Gourvenec, S., and Gottardi, G. (2010). "Centrifuge modelling of circular shallow foundations on sand." *International Journal of Physical Modelling in Geotechnics*, 10(2), 35-46.

Green, A. P. (1954). "The plastic yielding of metal junctions due to combined shear and pressure." *Journal of the Mechanics and Physics of Solids*, 2(3), 197-211.

Hansen, J. B. (1970). "A revised and extended formula for bearing capacity." Bulletin no. 28, Danish Geotechnical Institute, Copenhagen, 5-11.

Houlsby, G. T., and Cassidy, M. J. (2002). "A plasticity model for the behaviour of footings on sand under combined loading." *Géotechnique*, 55(2), 117-129.

IS456 (2000). "Plain and Reinforced Concrete - Code of Practice." Bureau of Indian Standard, New Delhi.

IS1893 (2016). "Crieteria for Eathquake Resistance Design of Structures, Part 1 General Provisons and Buildings ", Bureau of Indian Standard, New Delhi.

IS6403 (1986). "Code of Practice for Determination of Bearing Capacity of Shallow Foundations."Bureau of Indian Standards, New Delhi.

IS13920 (2016). "Ductile Detailing of Reinforced Concrete Structures Subjected to Seismic Forces - Code of Practice." Bureau of Indian Standard, New Delhi.

Keawsawasvong, S., and Ukritchon, B. (2017). "Undrained limiting pressure behind soil gaps in contiguous pile walls." *Computers and Geotechnics*, 83, 152-158.

Kim, D., Youn, J., Jee, S., Choi, J., Lee, J., and Choo, Y. (2014). "Numerical studies on combined VH loading and inclination factor of circular footings on sand." *Journal of the Korean Geotechical Society*, 30(3), 29-46.

Kim, D., Youn, J., Jee, S., and Choo, Y. (2014). "Numerical studies on combined VM loading and eccentricity factor of circular footings on sand." *Journal of the Korean Geotechical Society*, 30(3), 59-72.

Krabbenhoft, K., Lyamin, A., and Krabbenhoft, J. (2016). *OptumG2: Theory*, Optum Computational Engineering, Available on: www.optumce.com.

Krabbenhoft, S., Damkilde, L., and Krabbenhoft, K. (2012). "Lower-bound calculations of the bearing capacity of eccentrically loaded footings in cohesionless soil." *Canadian Geotechnical Journal*, 49(3), 298-310.

Loukidis, D., Chakraborty, T., and Salgado, R. (2008). "Bearing capacity of strip footings on purely frictional soil under eccentric and inclined loads." *Canadian Geotechnical Journal*, 45(6), 768-787.

Makrodimopoulos, A., and Martin, C. M. (2006). "Lower bound limit analysis of cohesive-frictional materials using second-order cone programming." *International Journal for Numerical Methods in Engineering*, 66(4), 604-634.

Makrodimopoulos, A., and Martin, C. M. (2007). "Upper bound limit analysis using simplex strain elements and second-order cone programming." *International Journal for Numerical and Analytical Methods in Geomechanics*, 31(6), 835-865.

Martin, C. M., and Houlsby, G. T. (2000). "Combined loading of spudcan foundations on clay: laboratory tests." *Géotechnique*, 50(4), 325-338.

Meyerhof, G. G. (1963). "Some recent research on the bearing capacity of foundations." *Canadian Geotechnical Journal*, 1(1), 16-26.

Montrasioa, L., and Nova, R. (1997). "Settlements of shallow foundations on sand: Geometrical effects." *Géotechnique*, 47(1), 49-60.

NCHRP (2008). "Report 611: Seismic Analysis and Design of Retaining Walls, Buried Structures, Slopes, and Embankments." National Cooperative Highway Research Program, Transportation Research Board, Washington, D.C.

NCHRP (2010). "Report 651: LRFD Design and Construction of Shallow Foundations for Highway Bridge Structures." National Cooperative Highway Research Program, Transportation Research Board, Washington, D.C.

Nguyen, D. L., Ohtsuka, S., and Kaneda, K. (2015). "Ultimate bearing capacity of footing on sandy soil against combined load of vertical, horizontal and moment loads." *Fifth International Conference on Geotechnique, Construction Materials and Environment,* Osaka, Japan.

Nova, R., and Montrasioa, L. (1991). "Settlements of shallow foundations on sand." *Géotechnique*, 41(2), 243-256.

OptumG2. 2018. Optum Computational Engineering, Copenhagen NV, Denmark.

Paolucci, R., and Pecker, A. (1997). "Seismic bearing capacity of shallow strip foundations on dry soils." *Soils and Foundations*, 37(3), 95-105.

Raj, D., Singh, Y., and Shukla, S. K. (2018). "Seismic bearing capacity of strip foundation embedded in $c$-$\phi$ soil slope." *International Journal of Geomechanics*, 18(7).

SAP2000. 2018. Computers and Structures Inc., Berkeley.

Shen, Z., Feng, X., and Gourvenec, S. (2016). "Undrained capacity of surface foundations with zero-tension interface under planar V-H-M loading." *Computers and Geotechnics*, 73, 47-57.

Sloan, S. W. (2013). "Geotechnical stability analysis." *Géotechnique*, 63(7), 531-572.

Taiebat, H. A., and Carter, J. P. (2000). "Numerical studies of the bearing capacity of shallow foundations on cohesive soil subjected to combined loading." *Géotechnique*, 50(4), 409-418.

Taiebat, H. A., and Carter, J. P. (2010). "A failure surface for circular footings on cohesive soils." *Géotechnique*, 60(4), 265-273.

Tang, C., Phoon, K.-K., and Toh, K.-C. (2014). "Effect of footing width on $N\gamma$ and failure envelope of eccentrically and obliquely loaded strip footings on sand." *Canadian Geotechnical Journal*, 52(6), 694-707.

Terzaghi, K. (1943). *Theoretical soil mechanics*, John Wiley & Sons, Inc., New York, USA.

Ukritchon, B., Whittle, A. J., and Sloan, S. W. (1998). "Undrained Limit Analyses for Combined Loading of Strip Footings on Clay." *Journal of Geotechnical and Geoenvironmental Engineering*, 124(3), 265-276.

Vesić, A. S. (1975). "Bearing capacity of shallow foundations." *Foundation Engineering Handbook, 1st edition*, H. F. Winterkorn, and H. Y. Fang, eds., Chapter 3, Van Nostrand Reinhold Company, Inc., New York, 121-147.

Vulpe, C., Gourvenec, S., and Power, M. (2014). "A generalised failure envelope for undrained capacity of circular shallow foundations under general loading." *Géotechnique Letters*, 4(3), 187-196.

Xiao, Z., Tian, Y., and Gourvenec, S. (2016). "A practical method to evaluate failure envelopes of shallow foundations considering soil strain softening and rate effects." *Applied Ocean Research*, 59(Supplement C), 395-407.

Yilmaz, M. T., and Bakir, B. S. (2009). "Capacity of shallow foundations on saturated cohesionless soils under combined loading." *Canadian Geotechnical Journal*, 46(6), 639-649.

Yun, G., and Bransby, M. F. (2007). "The horizontal-moment capacity of embedded foundations in undrained soil." *Canadian Geotechnical Journal*, 44(4), 409-424.